THE JOURNAL OF PHYSICAL CHEMISTRY B LETTERS

2005, *109,* 20669−20672
Published on Web 10/15/2005

Role of Stress in the Self-Limiting Oxidation of Copper Nanoparticles

Chun-Hua Chen, Tomohiko Yamaguchi, Ko-ichi Sugawara, and Kenji Koga*

Nanotechnology Research Institute, National Institute of Advanced Industrial Science and Technology, 1-1-1 Higashi, Tsukuba, Ibaraki 305-8565, Japan

Received: August 18, 2005; In Final Form: September 30, 2005

The oxidation process of Cu nanoparticles has been investigated by means of an in-situ X-ray diffraction method. A self-limiting oxidation process involving an unusually drastic decrease (about 4 orders in magnitude) in the oxidation rate was observed at 298 K, whereas a non-self-limiting oxidation emerged at 323 K with a rate of at least 4 orders in magnitude faster than 298 K. The drastic slowing at 298 K and the big differences between the two close temperatures in the oxidation kinetics were found to be directly correlated to whether the compressive stress in the $Cu_2O(111)$ layers that commensurately formed on the Cu(111) surface is relaxed or not.

The oxidation of bulk Cu surfaces has been investigated for over a century, as summarized in several books and reports,[1−3] whereas only a small number of works on the oxidation of the nanoparticulate Cu have been reported.[4−7] According to the results of the previous studies, Cu nanoparticles show more temperature-sensitive oxidation behaviors[5] and have much thinner surface oxides than bulk surfaces.[6,7] Only a slight change in the surface oxide thickness can significantly affect physical and chemical properties of nanoparticles due to the large surface-to-volume ratio when applied to conductors,[6] catalysts,[8] optical devices,[4] etc. To achieve the precise control of the oxide thickness as well as the oxidation rate for optimal performance of the devices, quantitative data on the oxidation kinetics of nanoparticles is of critical importance but is lacking at present. In this Letter, we report quantitative experimental results on the oxidation kinetics of Cu nanoparticles and their temperature dependences via an in-situ X-ray diffraction (XRD) method. Our results provide a greater understanding of how the bulk surface oxidation changes by the finite-size effect.

The Cu nanoparticles were generated by cooling the Cu vapor from a high purity ingot (99.9999%) at 1393 K with purified helium in a vacuum chamber. They were immediately transported with a helium flow through a stainless steel tube and deposited on an MgO(100) substrate (at 298 K) that was placed in another vacuum (specimen) chamber on an X-ray diffractometer. An X-ray beam passed through a carbon window of the specimen chamber to the substrate surface fixed at a 2° grazing-incidence angle. A high-power 18 kW Cu rotating anode X-ray source was employed to obtain good quality data. The diffracted beam was monochromatized to Cu K_α by a HOPG crystal and detected by a scintillation counter. The instrumental performance has been quantitatively verified in our previous work.[9]

To observe the initial oxidation process via XRD, we introduced dry air into the specimen chamber with keeping its pressure at 14 Pa by means of a rotary pump during which a batch scan ($2\theta = 20-60°$ for ~1 h) was performed repeatedly. After a 70 h measurement, we found almost no change among successively recorded XRD patterns and then increased the pressure to 9.3×10^4 Pa to detect the further oxidation for another 120 h. The above measurements were taken while the sample temperature was maintained at 298 K. Another XRD experiment was performed at 323 K. To see the morphology and size distribution, Cu nanoparticles were deposited on a holey carbon microgrid and transferred in air to a 200 kV high-resolution electron microscope (HREM), JEOL JEM-2010 with a 0.194 nm point-to-point resolution. Icosahedral particles dominated under our growth conditions, as seen in the inset of Figure 1. The volume-mean sizes of the XRD samples on the measurements at 298 and 323 K were 14 and 11 nm, respectively. Scanning electron microscope (SEM) images from the XRD samples showed particles stacked in a fairly porous fashion. The Brunauer−Emmett−Teller (BET) surface area at 298 K showed 18 $m^2\ g^{-1}$, denoting a 62% reduction from the isolated state, and no remarkable growth was detected at 323 K.

From the partially enlarged HREM image in Figure 1, the lattice fringes at the particle inside are attributed to Cu(111) with a spacing of 0.209 nm, whereas those at the near surface region show a larger spacing of 0.25 nm, corresponding to $Cu_2O(111)$. This indicates the $Cu_2O(111)//Cu(111)$ epitaxial relation, which has been observed on the bulk Cu(111) surface.[1] Figure 2a shows the XRD pattern of the as-deposited Cu nanoparticles under a vacuum (10^{-4} Pa), and parts b−e of Figure 2 illustrate several raw data measured during the air exposure at 298 K. Figure 2f displays the final spectrum at 323 K. The peak positions observed can be indexed to Cu and Cu_2O with no CuO peak. The absence of the Cu_2O 111 peak in Figure 2a indicates a trace level of the oxide below the detection limit before oxidation.

The integrated intensities of Cu_2O 111 and Cu 111 and the lattice parameters of both phases were derived by profile-fitting procedures using four asymmetrical pseudo-Voigt functions for

* Corresponding author. E-mail: k.koga@aist.go.jp.

10.1021/jp0546498 CCC: $30.25

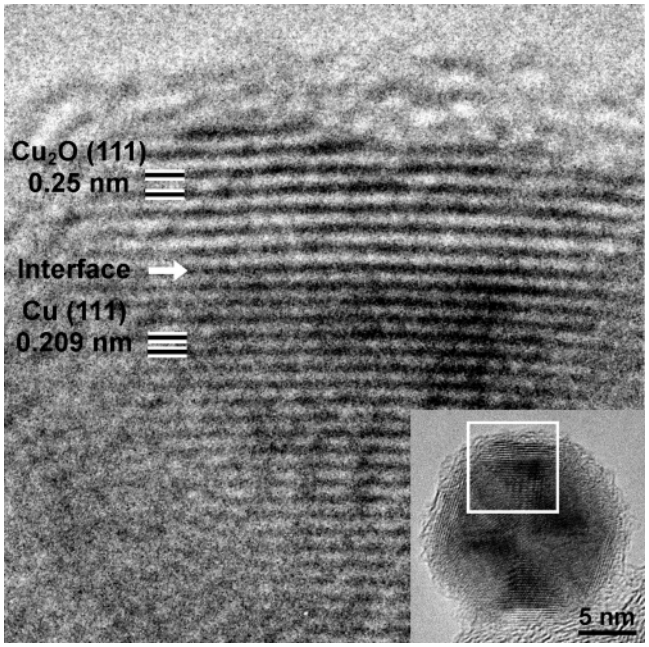

Figure 1. Typical HREM image of an icosahedral Cu nanoparticle (~16 nm) with $Cu_2O(111)$ surface oxide layers (6−7 ML).

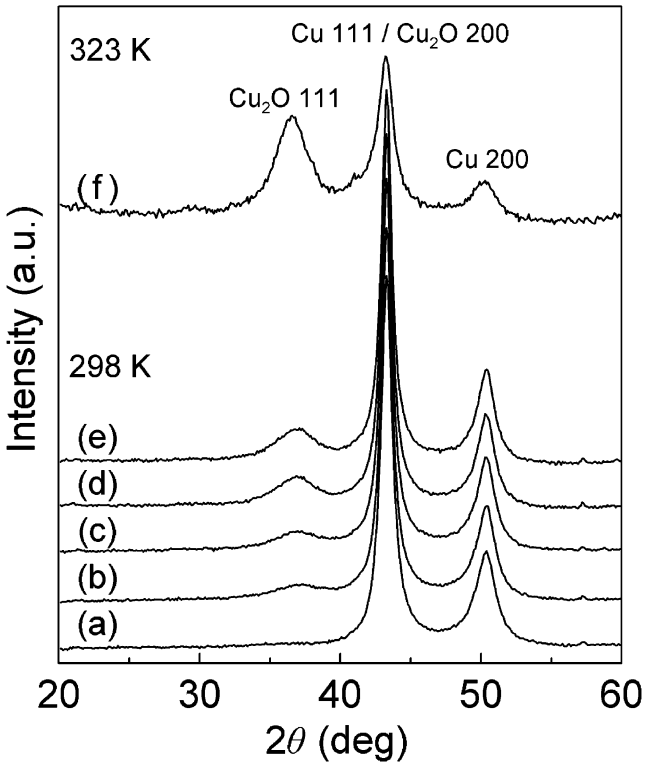

Figure 2. X-ray diffraction patterns (Cu K_α) of Cu nanoparticles (a) before oxidation, and after exposing dry air at 298 K for (b) 10 h (14 Pa), (c) 20 h (14 Pa), (d) 70 h (14 Pa) + 10 h (9.3×10^4 Pa), (e) 70 h (14 Pa) + 120 h (9.3×10^4 Pa) and at 323 K for (f) 70 h (14 Pa) + 120 h (9.3×10^4 Pa).

111 and 200 peaks of Cu_2O, and those of Cu.[10] To coordinate the air exposure time at 14 Pa with those at 9.3×10^4 Pa, we examined the pressure dependence of the oxidation kinetics in a supplemental experiment. Because Cu_2O is a well-known p-type oxide, the oxidation of Cu is governed by the outward diffusion of Cu ions via Cu vacancy sites generated by the chemisorbed oxygen dissolution. The concentration of Cu vacancies as well as the oxidation rate thus depends on the ambient oxygen pressure in the $P_{O_2}^{1/n}$ form.[11] The n value for Cu nanoparticles has never been reported before. We found that $n = \sim 1.5$, which is much smaller than that of bulk surfaces ($n \geq 4$ in general).[11−13] This indicates that the nanoparticle surface is much more sensitive to the oxygen pressure, though the detail defect mechanism for $n = 1.5$ is not clear. The air exposure time at 14 Pa was then converted to that at 9.3×10^4 Pa by means of the equation of $P_{O_2}^{1/1.5}t =$ constant. The intensity ratio was converted to the volume fraction (x) of Cu oxidized, as shown in Figure 3, by using Cu and Cu_2O structure factors and their Debye parameters.[14] The average oxide thickness (L) was then calculated from the volume fraction and the BET analysis result by assuming the form of a spherical metal core with an oxide shell. The derived final thickness at 298 K, 2.3 nm (9.2 ML), is in good agreement with the HREM observation of 7−9 ML, as shown in Figure 1.[15] In contrast, the volume fraction at 323 K reaches a higher value at the end of the experiment and still continues to increase.

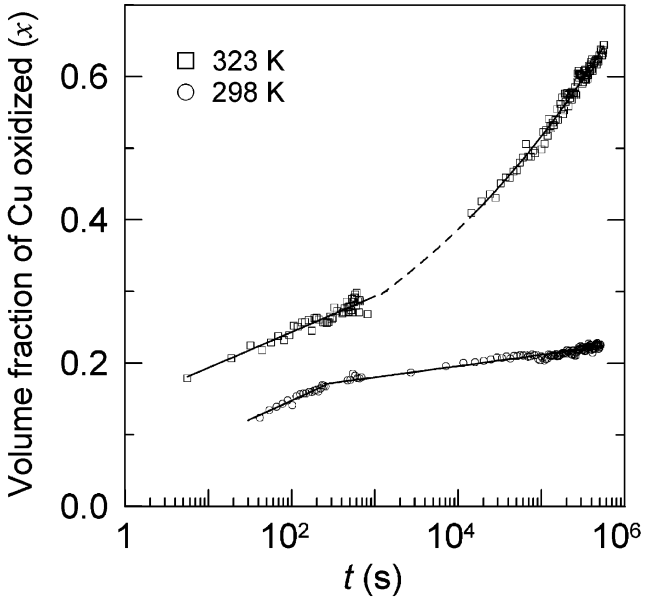

Figure 3. Volume fraction of Cu oxidized (x) versus the air exposure time at a pressure of 9.3×10^4 Pa on a linear-log scale for the 298 and 323 K data. The solid lines are drawn based on the data analysis results (see text).

We analyzed the plot of L versus t in view of basic rate laws for the oxidation kinetics,[1] i.e., logarithmic, inverse-logarithmic, linear, parabolic, cubic, and higher power rate laws. At lower temperatures and in thin oxide films, the inverse-logarithmic equation based on the theory by Cabrera and Mott[16] has often been employed to explain the oxidation kinetics of Cu bulk surfaces.[1−3,17] But our data at both temperatures could not be fitted with this equation. The only equation that fit the data at 298 K was found to be direct-logarithmic, $dL/dt = k \exp(-L/L_0)$, where t is the exposure time at 9.3×10^4 Pa air pressure, k is the rate constant, and L_0 is constant. In addition, the oxidation process at 298 K could be clearly divided into two stages that can also be seen in Figure 3, because the linear relationship between x and L is well established at the thinner oxide state. The rate constants were then estimated to be $k^{(1)}_{298K} = 1.9 \times 10^{-2}$ nm s^{-1} for $L < 7.0$ ML ($x < 0.17$) (first stage) and $k^{(2)}_{298K} = 7.3 \times 10^{-6}$ nm s^{-1} for $L > 7.0$ ML (second stage). It is surprising to note that the rate constant at the first stage dropped 4 orders of magnitude at the second stage. The second stage rate constant denotes only a ~1 ML increase after 1 year, which is an indication of the self-limiting oxidation.[18] In the case of 323 K, the data at the thinner state, $L < 9.6$ ML ($x <$

0.29), was also best fitted by the direct-logarithmic function with the rate constant $k^{(1)}_{323K} = 4.2 \times 10^{-2}$ nm s^{-1}. At the thicker state ($x > 0.29$), the relation between x and L starts to deviate from the linear relationship. Thus, we employed the modified parabolic law derived from a spherical particle model[19] to obtain $k^{(2)}_{323K} = 2.9 \times 10^{-7}$ nm^2 s^{-1}. Here we can briefly conclude that at the initial thinner state (described by $k^{(1)}$), the oxidation at both 298 and 323 K follows the direct-logarithmic rate law. It is reliable that $k^{(1)}_{323K}$ is only slightly larger than $k^{(1)}_{298K}$ due to the small temperature difference, and both of them are comparable with the value of $\sim 3 \times 10^{-2}$ nm s^{-1} obtained for the bulk surface at room temperature,[29] suggesting the size effect is absent at the thinner state. It should be noted that the slightly different initial states afterward undergo considerably different oxidation kinetics between the two close temperatures.

Parts a and b of Figure 4 show the Cu_2O and Cu lattice constant variations versus t at 298 and 323 K, respectively.[20] At the very initial oxidation stage, the Cu_2O lattice constant at both temperatures shows a much smaller value than that of the bulk and quickly increases as the exposure time increases. A similar feature was also observed in the aqueous oxide on the Cu(111) surface.[21] At the end of the experiments, the Cu_2O lattice constant at 298 K was 1.1% smaller than the bulk value, whereas the lattice constant at 323 K showed a value that was only 0.33% smaller. The previous studies of the Cu(111) surface oxidation provide us important information regarding the present icosahedral particles with only (111) facets. According to the XRD[21] and RHEED[22] studies, $Cu_2O(111)$ is formed on Cu(111) with a 3−7 commensurate relation, where 3 times the O−O nearest-neighbor distance in $Cu_2O(111)$ is commensurate with 7 times the Cu−Cu distance in Cu(111) along $\langle 1\bar{1}0 \rangle$ directions. In the 3−7 commensurate Cu_2O structure, the in-plane lattice spacing contracts 1.16% from the bulk value, which corresponds to the 0.422 nm lattice constant. As can be seen in Figure 4a, the Cu_2O lattice constant at 298 K is trapped at ~0.422 nm (3−7 structure) from 6.4 ML ($t >$ ~130 s) up to the final oxide thickness of 9.2 ML. In the case of 323 K, the Cu_2O lattice constant exceeds that of the 3−7 structure at ~9 ML and approaches the bulk value as the oxidation proceeds (see Figure 4b). In addition, the core Cu lattice was found to contract at both temperatures when the thin oxide film (<~9 ML) formed, suggesting the internal pressure increased by the oxide shell. As the oxide thickness increased further at 323 K, the Cu core started to relax.

Why does the oxidation process change so drastically between the two close temperatures? This difference could not be explained by the temperature change itself because only an 8% change in temperature does not lead to such a great enhancement of the Cu vacancy concentration and the Cu ion diffusivity. The Cu_2O stress condition, as found in Figure 4a, can be considered to play an important role in the oxidation behavior as follows. It is known that the ion diffusion coefficient can be affected by the stress in the form $D = D_0 \exp(-pv/k_BT)$, where D_0 is at the stress-free state, p the hydrostatic pressure, v the activation volume, k_B the Boltzmann constant, and T the temperature.[23] When the Cu_2O lattice is isotropically contracted to have the in-plane lattice spacing of the 3−7 structure, a compressive pressure becomes 3.6 GPa from the relationship $\Delta p = 3(\Delta a/a)/\kappa$ with the Cu_2O compressibility[24] $\kappa = 9.3 \times 10^{-12}$ m^2 N^{-1}. Assuming an activation volume[25] in the range 10^{-3} to 10^{-2} nm^3, the 3.6 GPa compressive pressure leads to a drastic decrease in the diffusion coefficient on the order of 10^{-1} to 10^{-4}. The drastic change of about 4 orders in magnitude in the rate constant between $k^{(1)}_{298K}$ and $k^{(2)}_{298K}$, as well as $k^{(2)}_{298K}$ and $k^{(1)}_{323K}$, can be explained by this estimation. The 3−7 structure starts to form from 6.4 ML (see Figure 4a), which is almost in agreement with the depression that occurs from 7.0 ML (see Figure 3). Regarding the strong correlation between Figures 3 and 4, the self-limiting oxidation at 298 K is considered to originate from the compressive stress accumulated in the 3−7 Cu_2O shell, structured by anchoring to the Cu(111) surface. The system gains enough thermal energy at 323 K to relax the compressive stress caused by the 3−7 structure. Although the stress effects on the oxidation rate produced by epitaxy were previously predicted by Fromhold,[26] there has never been direct experimental evidence for them. Our experiments provide a clear result to conclude that the stress plays a critical role in the oxidation of metal nanoparticles.

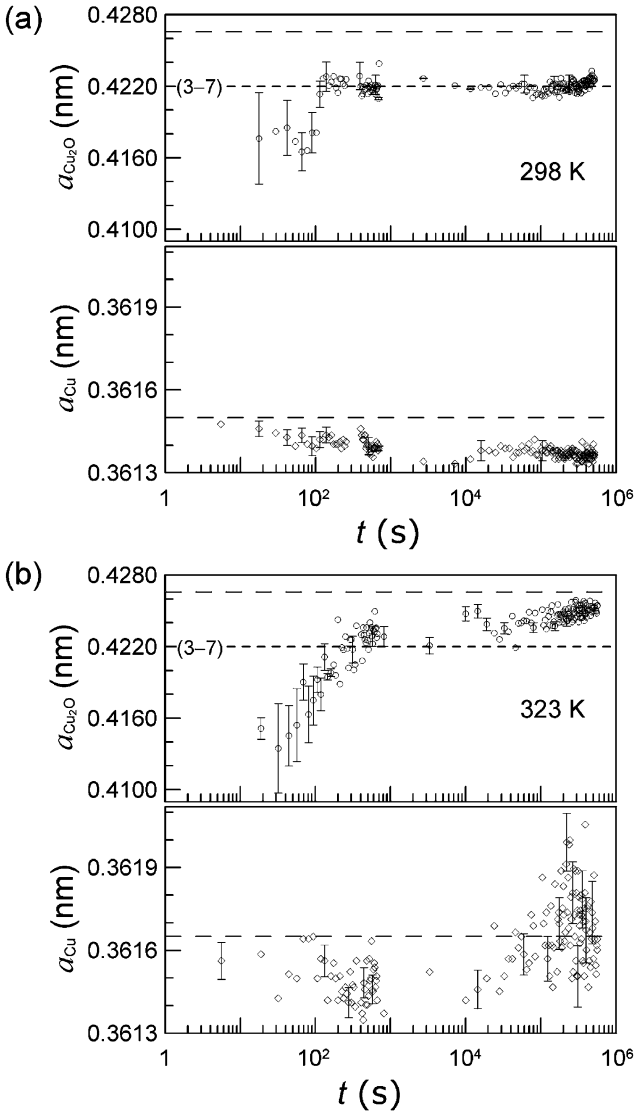

Figure 4. Cu_2O and Cu lattice constants, a_{Cu_2O} and a_{Cu}, versus the air exposure time at the pressure of 9.3×10^4 Pa, at (a) 298 K and (b) 323 K. The long dash lines denote the Cu_2O and Cu bulk lattice constants, where those at 323 K were derived with the linear thermal expansion coefficients. The short dash line denotes a lattice constant corresponding to the 3−7 commensurate structure of $Cu_2O(111)$ layers on Cu(111).

As argued above, the ion current is strongly affected by the internal stress in the thinner oxide (<~9 ML), resulting in the drastic rate-depression. The kinetics in such a thin region were found to be ruled by the direct-logarithmic law. There are some theories demonstrating this law when rate-limitation by tunneling

electron current is assumed,[27] by trapped electrons at lattice defect sites[28] or by ion transport.[12] From our results alone, however, the most appropriate mechanism cannot be fixed. Even if the electrons play an important role in limiting the rate, their current might be influenced by the ion current depression due to the role of the charge neutrality condition, whereas the parabolic kinetics[1] found at the thicker oxide state (>9.6 ML) have been commonly observed in the thick oxide films and at higher temperatures. This feature suggests that the ions truly start to dominate as the rate-limiting species at such a thicker region.

The first stage oxidation rate of Cu nanoparticles at 298 K shows a value comparable to that of the film surface.[29] Nevertheless, the oxidation stops at the thinner critical thickness (~2 nm) on the nanoparticle surface than on the macroscopic surface, e.g., ~5 nm.[29] Ho and Vook showed that the Cu_2O-(111) layers at 623 K can keep the 3−7 structure on the Cu-(111) surface up to ~5 ML and then relax by generation of misfit dislocations in further oxidation.[22] Thus, the difficult oxidation of Cu nanoparticles at 298 K might originate from the lack of such a relaxation mechanism because of the effect of the nanoscaled surface area.

In conclusion, we have quantitatively observed the oxidation kinetics of Cu nanoparticles and their temperature dependences. The oxidation behavior (self-limiting or non-self-limiting) was found to be directly related to the stress condition in the oxide shell. The present result should provide valuable data for the understanding of the self-limiting oxidation kinetics of metal nanoparticles and also for the control of their oxide thickness.

Acknowledgment. This work was supported in part by the Shorai Foundation for Science and Technology.

References and Notes

(1) Rönnquist, A.; Fischmeister, H. *J. Inst. Met.* **1960**−**1961**, *89*, 65.
(2) Hauffe, K. *Oxidation of Metals*; Plenum Press: New York, 1965.
(3) Fromhold, A. T. *Theory of Metal Oxidation*; North-Holland: New York, 1976.
(4) Yanase, A.; Matsui, H.; Tanaka, K.; Komiyama, H. *Surf. Sci.* **1989**, *219*, L601.
(5) van Wijk, R.; et al. *Appl. Surf. Sci.* **1995**, *90*, 261.
(6) Kozhevin, V. M.; et al. *Phys. Solid State* **2003**, *45*, 1993.
(7) Tamura, K.; et al. *Jpn. J. Appl. Phys.* **2003**, *42*, 7489.
(8) Arul Dhas, N.; Paul Raj, C.; Gedanken, A. *Chem. Mater.* **1998**, *10*, 1446.
(9) Koga, K.; Takeo, H. *Rev. Sci. Instrum.* **1996**, *67*, 4092. Koga, K.; Takeo, H.; Ikeda, T.; Ohshima, K. *Phys. Rev. B* **1998**, *57*, 4053.
(10) The 2θ position and integrated intensity of the hidden Cu_2O 200 peak in the Cu 111 was fixed in the fitting procedure regarding the separated Cu_2O 111 position.
(11) Wagner, C.; Grünewald, K. *Z. Phys. Chem.* **1938**, *40*, 455.
(12) Grimley, T. B.; Trapnell, B. M. W. *Proc. R. Soc.* **1956**, *A234*, 405.
(13) Roy, S. K.; Bose, S. K.; Sircar, S. C. *Oxidation Met.* **1991**, *35*, 1.
(14) Wilson, A. J. C., Ed. *International Tables for X-ray Crystallography*; Kluwer-Academic Press: Netherlands, 1992; Vol. C, p 500. Böhmer, W.; Rabe, P. *J. Phys. C* **1979**, *12*, 2465.
(15) From a supplemental experiment, we found that the X-ray radiation from a Cu anode at 45 kV and 300 mA gives an additional increase (~40%) in the oxide volume at 298 K. The 298 K critical oxide thickness without the irradiation effect was thus estimated to be ~1.6 nm (6.4 ML).
(16) Cabrera, N.; Mott, N. F. *Rep. Prog. Phys.* **1948**, *12*, 163.
(17) Fromhold, A. T.; Anderson, M. H. *Oxidation Met.* **2004**, *62*, 237.
(18) We confirmed that the self-limiting oxidation behavior was unaffected when dry air was directly exposed at 9.3×10^4 Pa to unoxidized particles.
(19) Carter, R. E. *J. Chem. Phys.* **1961**, *34*, 2010.
(20) To correct systematic errors on the lattice constant determinations, the bulk Cu lattice constant was applied to the Cu 111 position before oxidation because of the sufficiently large sizes of the present particles: Montano, P. A.; et al. *Phys. Rev. Lett.* **1986**, *56*, 2076. The Cu and Cu_2O lattice constants during oxidation were then determined by correcting the Cu 111 and Cu_2O 111 positions with a 2θ correction factor because the two peaks are closely located.
(21) Chu, Y. S.; Robinson, I. K.; Gewirth, A. A. *J. Chem. Phys.* **1999**, *110*, 5952.
(22) Ho, J. H.; Vook, R. W. *J. Cryst. Growth* **1978**, *44*, 561.
(23) Kao, D.-B.; McVittie, J. P.; Nix, W. D.; Saraswat, K. C. *IEEE Trans. Electron. Devices* **1988**, *35*, 25.
(24) Hallberg, J.; Hanson, R. C. *Phys. Status Solidi* **1970**, *42*, 305.
(25) Perriat, P.; Domenichini, B.; Gillot, B. *J. Phys. Chem. Solids* **1996**, *57*, 1641.
(26) Fromhold, A. T. *J. Appl. Phys.* **1965**, *36*, 865.
(27) Mott, N. F. *Trans. Faraday Soc.* **1940**, *36*, 472.
(28) Uhlig, H. H. *Acta Met.* **1956**, *4*, 541.
(29) White, A. H.; Germer, L. H. *Trans. Electrochem. Soc.* **1942**, *81*, 305.